Technical Paper

ISSN 1997-1400 Int. J. Pavement Res. Technol. 3(4):207-215

Benefit Analysis of Permeable Pavement on Sidewalks

Dan-Chi Wang[1+], Lung-Chang Wang[2], Kuang-Yen Cheng[3], and Jyh-Dong Lin[4]

Abstract: The benefit of incorporating permeable pavement into sidewalks in Taipei was analyzed with respect to hydrological and thermal considerations. To date, a six-month, on-site monitoring program has been carried out to evaluate the capability of sidewalks with permeable pavement to suppress surface runoff, recharge groundwater, and lower the ground surface temperature during rainstorms. Additionally, the duration of ground-surface temperature effects has also been evaluated. The field results showed that, when the precipitation was below 35*mm*, the infiltration efficiency exceeded 80%, while the surface temperature of the permeable pavement decreased continually for two days if the ambient temperature was from 19 to 23°C.

Key words: *Heat island effect; Infiltration; Permeable pavement; Surface runoff.*

Introduction

Urbanization greatly reduces the percentage of permeable surface in municipal areas because massive, artificial, waterproof surface replaces natural vegetation, which would normally facilitate the percolation of rainwater into the ground. During a rainstorm, the increased surface runoff may cause flooding by overloading the drainage system and the river. Additionally, impermeable surfaces impede cooling of the ground surface temperature by hindering the evaporation of moisture that has been trapped in the underlying soil. Therefore, an increased impermeable area will contribute to the elevated ground surface temperatures and dryness commonly seen in highly urbanized regions.

During the urbanization process, increases in population and infrastructure density cause significant changes in surface runoff and in the arrival times of peak currents and peak flooding. Increasing the extent of impermeable surface prevents effective percolation of the rainwater into the ground, thus leading to frequent flooding from excessive surface runoff [1]. Moreover, the unique climate pattern of a metropolis has turned out to be a social problem. The higher temperature in a metropolis is referred to as the “heat island effect” and is associated with the high density of high-rise buildings, the reduction of tree area, and the increased heat generation from energy consumption among many other factors [1]. The amount of paved, impermeable surface in a metropolis is a major cause of the heat island effect. Materials commonly used in urban areas, such as concrete and asphalt, have higher heat capacity, thermal conductivity, and surface radiative properties (albedo and emissivity) than do unpaved surfaces. These differences in thermal properties cause changes in the energy balance of urban areas, often leading to higher temperatures than in the surrounding rural areas. The energy balance is also affected by the lack of vegetation in urban areas that would normally promote cooling by evapotranspiration [1]. The asphalt and concrete that cover paved surface also suppress moisture evaporation, and the ground temperature rises easily, especially during summer. Therefore, improving the thermal characteristics of the pavement is of great importance in maintaining a good thermal environment in a metropolis.

The advantages of adopting water-permeable sidewalks for improving the urban environment are summarized as follows [2-4]:

1. Rainwater can penetrate rapidly to recharge the groundwater.
2. Increased penetration of water and air help keep the underlying ground stable.
3. Permeable pavement offers a safer sidewalk for pedestrians because it does not accumulate water, which can pose a splash hazard during the day and a reflection hazard at night.
4. The permeable sidewalk assists in adjusting the surrounding ground temperature and humidity to alleviate the heat island effect in the city.

The U.S and Japan have already conducted research on using water-permeable surface materials to solve problems resulting from urbanization since the 1980s. This paper presents the benefits of water-permeable surfaces with respect to thermal and hydrological metrics by analyzing field data from a water-permeable sidewalk installed in Taipei.

Case Study of Permeable Pavement on Sidewalks at Bei-An Road, Taipei

Site Location

The experimental site is located at the south side of Bei-An Road. The pavement on the sidewalk had been seriously damaged and urgently needed repairs. On the south side of the site, there is a river bank, and there are no inhabitants or business activities between the sidewalk and the river bank. On the north side of Bei-An Road, are the Grand Hotel, Radio Taiwan International, the Hero Shrine, the military police corps, and Bei-An junior high school. Therefore, there are fewer pedestrians and vehicles utilizing the south side. Thus, the field study was not expected to cause much inconvenience

[1] PhD Candidate, College of Engineering, National Taipei University of Technology, Taipei 10608, Taiwan.
[2] Professor, Department of Civil Engineering, National Taipei University of Technology, Taipei 10608, Taiwan.
[3] Associate Professor, Department of Civil Engineering, National Taipei University of Technology, Taipei 10608, Taiwan.
[4] Professor, Department of Civil Engineering, National Central University, Taoyuan County 32001, Taiwan.
[+] Corresponding Author: E-mail wangdanchi@gmail.com
Note: Submitted August 3, 2009; Revised December 20, 2009; Accepted February 08, 2010.

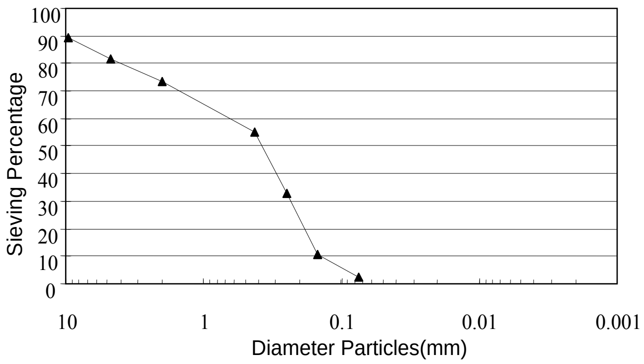

Fig. 1. Particles Analytic Curve.

Fig. 2. The Finished Surface of JW Structural Pervious Air-Circulated Aqueduct Concrete Pavement.

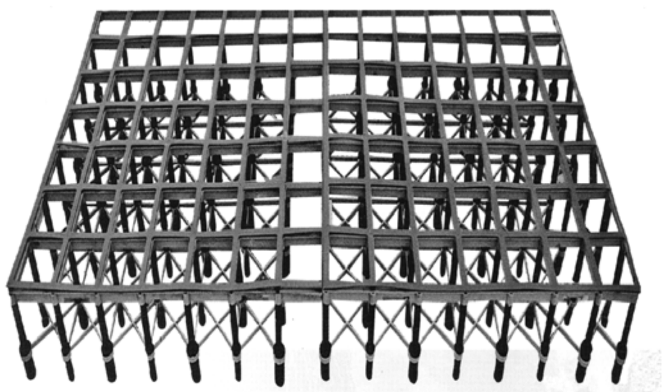

Fig. 3. The Structure of JW Structural Pervious Air-Circulated Aqueduct Concrete Pavement.

to pedestrians or traffic.

Experiment Design

Two strategies were taken to evaluate the benefit of water-permeable paving on-site. Monitoring instruments (water meter, rain gauge, geothermometer, and recorder) were first deployed at the experimental site to record long-term data on infiltration quantity, rainfall, and temperature changes. The pavement water retentivity and Guelph Permeameter rates were determined to evaluate the relationships among infiltration, surface runoff, temperature, and water content.

In addition, soil samples were collected at depths of 0.5-1.0*m* to analyze particle-size distribution [5]. A typical size distribution is shown in Fig. 1. The soil was classified as SP in accordance with the USCS (Unified Soil Classification System), and also as A-3 in accordance with the AASHTO (American Association of State Highway and Transportation Officials) system. The soil permeability coefficient measured on-site was approximately $6.83 \times 10^{-4} cm/s$.

Table 1. Material Specifications of Experiment Pavements.

Type	Material Specifications
Precast Permeable Brick Type A	Size：30×30×4*cm*. Inorganic Metallic Oxide or Mineral Substance. Ex: Feldspar, Clay. With High Pressure Forming, High Pressure Liquefaction Sintering. Anti-acid and Anti-alkaline.
Precast Permeable Brick Type B	Size：30×30×4*cm*. Recycled Ceramics, Recycled Glass, Sewer Sludge, Reservoir Silt, and Agglutinant, Adhesive and Pigment.
Precast Permeable Brick Type C	Size：20×20×2.3*cm* and 10×10×2.3*cm*. Waste Recycled Condensed Ceramics Pellets Under High Temperature Porcelain and Ceramics Kiln Burns.
Precast Permeable Pavement Type D	Reinforced Concrete, Crack-proof Textile, and Integrated Surface.

Pavement Styles

To evaluate the benefits of various water-permeable pavements, four types of water-permeable pavements were tested and compared, and three of these four types consisted of different water-permeable bricks. These bricks (precast, permeable brick type A, B, and C) were made of recycled materials such as ceramics, glass, waste ore, sewer sludge, reservoir silt, and pigment bound together with agglutinant and adhesive as shown in Table 1 [6-10]. Another type of tested material was the special JW Structural Pervious Air-Circulated Aqueduct Concrete Pavement (precast permeable pavement type D), as shown in Fig. 2. It is a pavement constructed on-site that allows the surface runoff to infiltrate or evaporate so that the paved surface retains its natural characteristics (Table 1). The water conduit is made of a durable plastic material to resist UV (ultraviolet) light. The pavement was constructed to be linked in a modular fashion, and it was reinforced with crack-proof steel fibers in the cement. This results in a reinforced concrete that has significantly improved compression and bending strength. The plastic water conduit was embedded in the reinforced concrete so that the conduit was as durable as the concrete floor slab in Fig. 3.

The JW Structural Pervious Air-Circulated Aqueduct Concrete Pavement is composed of the air-cycle aqueduct frame, an aqueduct concrete structure layer and a water storage and pervious layer, as shown in Fig. 4. The pavement consists of the following components:

1. The main structure is the "Aqueduct concrete structure layer", which is cast as one piece using a special concrete. It is not made of porous pavement material because its primary purpose is to provide strength under pressure.

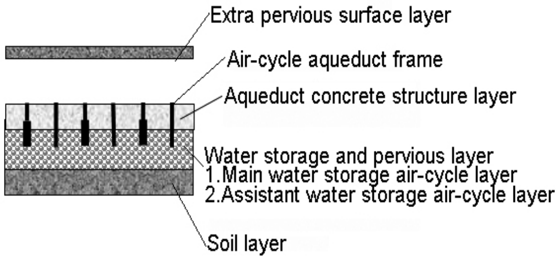

Fig. 4. Section of JW Structural Pervious Air-Circulated Aqueduct Concrete Pavement.

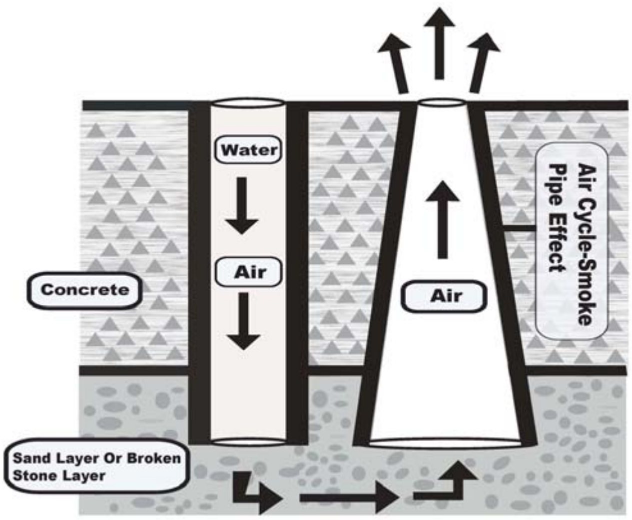

Fig. 5. Diagram of Initiative Air Circulation.

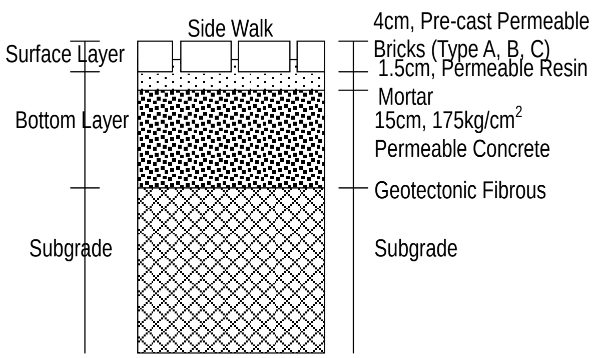

Fig. 6. Section of Permeable Pavement Type A, B, and C.

2. The "air-cycle aqueduct frame" is made of recycled plastic and is permeable by water and air. The aqueduct also serves as a reinforcing structure to increase the strength of the pavement when it is subject to tension and a bending moment.
3. The "water storage and pervious layer" consists of sand and aggregate layers with large porosity to allow the underlying soil to retain more water.

The J W Structural Pervious Air-Circulated Aqueduct Concrete Pavement has very good water-retention capability that allows the soil to retain more water. The "water-pervious and storage layer" has larger porosity to provide a larger space in which cool air can flow.

Moreover, the "air-cycle aqueduct frame" has a cone shape--the initial upward movement of cool air from underground forms air

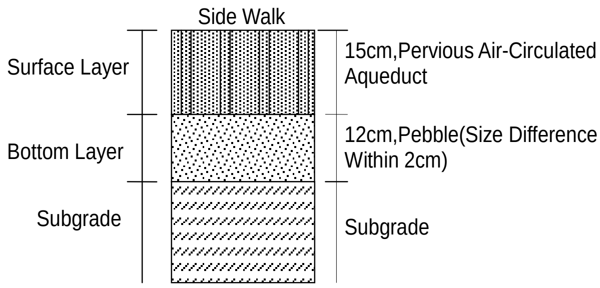

Fig. 7. Section of Permeable Pavement Type D.

Table 2. Compressive Strength and Water Permeability.

Type	Compressive Strength (*kg/cm*^{2})	Water Permeability Coefficient (*cm/s*)
Precast Permeable Brick Type A	≧240	1.0×10^{-1}
Precast Permeable Brick Type B	≧360	7.0×10^{-2}
Precast Permeable Brick Type C	≧430	2.2×10^{-4}
Precast Permeable Pavement Type D	≧360	Permeable

circulation patterns that assist in dramatically lowering the temperature of the ground surface (Fig. 5).

All three types of precast water permeable bricks are 20.5*cm* in thickness, including the surface and bottom layers. The J W Structural Pervious Air-Circulated Aqueduct Concrete Pavement is 27*cm* in thickness including the surface and bottom layer, as shown in Figs. 6 and 7.

The cross section of the precast permeable bricks type A, B, and C are shown in Fig. 6. The surface layer is 4*cm* thick on top of the 15-cm permeable concrete bottom layer that will support a 175*kg/cm*^{2} load. The total thickness is 20.5 *cm*, with a 15- cm permeable resin mortar between the surface and the bottom layers. Fig. 7 shows the cross section of the JW Structural Pervious Air-Circulated Aqueduct Concrete Pavement. Its surface layer is the 15-cm "pervious air-cycle aqueduct," cast with impermeable concrete for holding the upper end of the "air-cycle aqueduct frame" in place. It also serves as the paved road surface that has sufficient strength to resist compression. The bottom layer is 12*cm* of pebbles, and the total thickness is 27*cm*. The lower end of air-cycle aqueduct frame is embedded in the bottom layer (Fig. 7), thereby allowing rainwater to be drained from the air-cycle aqueduct frame directly into the subgrade. The data on compression resistance, pervious factor, and the material compositions are listed in Tables 1 and 2.

Experiment Results

Hydrology Benefit

Long-term rainfall and infiltration seepage have been monitored for six months. Hourly precipitations of six observed rainfalls are shown in Figs. 8 to 13. The results of the water-retention experiment are listed in Table 3, and the calculated infiltration efficiency and surface runoff efficiency (based on the data shown in Figs. 8 to 13

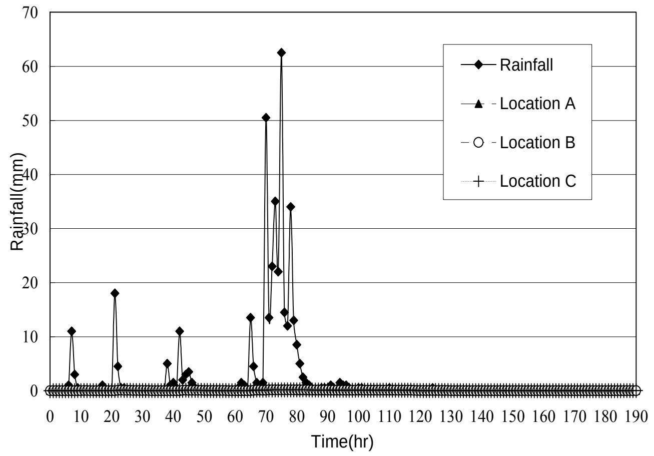

Fig. 8. Data of Rainfall No.1 on the Experiment Area.

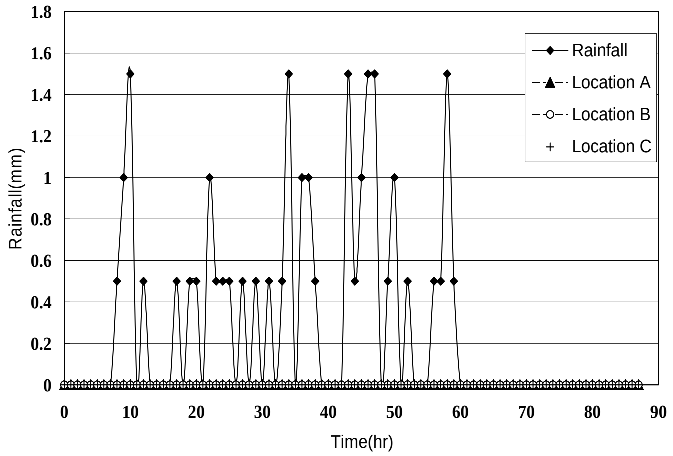

Fig. 11. Data of Rainfall No.4 on the Experiment Area.

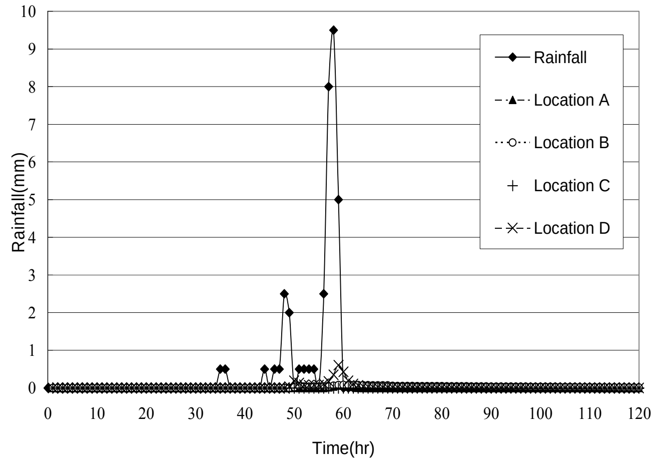

Fig. 9. Data of Rainfall No.2 on the Experiment Area.

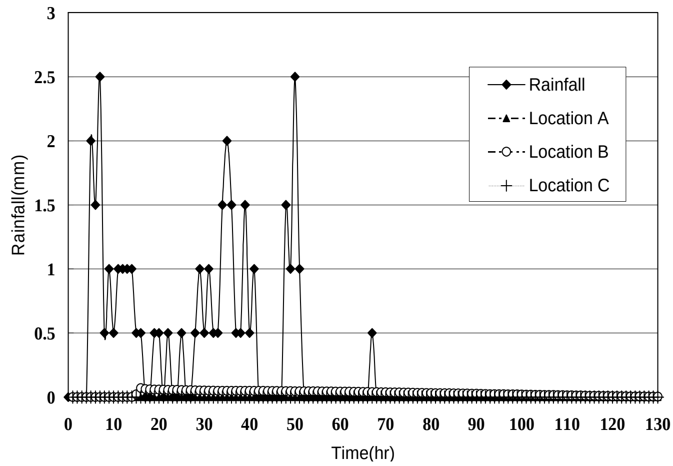

Fig. 12. Data of Rainfall No.5 on the Experiment Area.

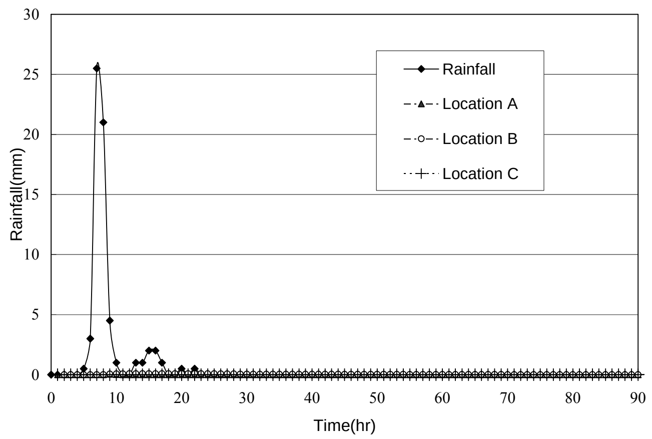

Fig. 10. Data of Rainfall No.3 on the Experiment Area.

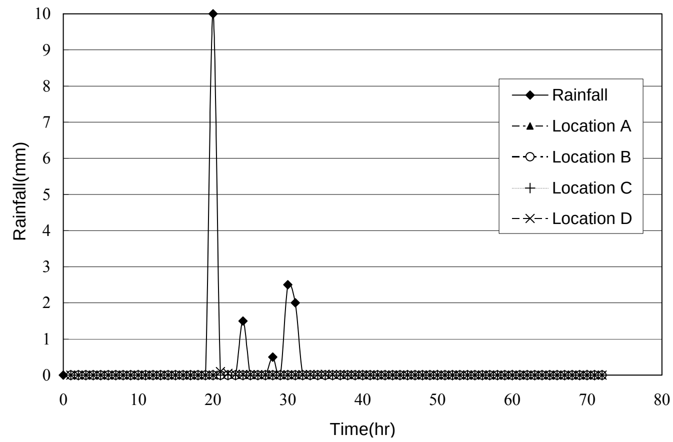

Fig. 13. Data of Rainfall No.6 on the Experiment Area.

and Table 3) are presented in Table 4. The water-permeable surface was effective in suppressing surface runoff and recharging groundwater after a rainstorm. For precipitation under 35 *mm*, the infiltration efficiency exceeded 80%.

Thermal Benefit

Thermal benefit, like hydrological benefit, is evaluated based on the long-term monitoring results. The data were collected in the four designated experimental areas with three geothermometers installed in the upper layer, under the upper layer, and in the bottom layer for each area. One additional geothermometer was placed outside the experimental area, with an additional thermometer on the asphalt concrete surface. The temperature for the surface of the upper layer and the surface of asphalt concrete are shown in Fig. 14, along with the outdoor ambient temperature. Changes of temperature are shown

Table 3. Precipitation Data.

No.	Recently Rain Field	Amount of Rain-fall(*mm*)	Exfiltration Amount(*mm*)	Exfiltration Efficiency (%)
No.1	65 Hours Ago (4.0mm Rainfall)	401.5	Location A：0.81 L Location B：10.47 Location Location C：0.00 L Location D：- Location	ocation A：0.20 B：2.61 ocation C：0.00 D：-
No.2	629 Hours Ago (1.5mm Rainfall)	34	Location A：0.27 L Location B：3.11 L Location C：0.00 L Location D：3.07 L	ocation A：0.79 ocation B：9.15 ocation C：0.00 ocation D：9.03
No.3	177 Hours Ago (1.5mm Rainfall)	63.5	Location A：0.04 L Location B：3.11 L Location C：0.00 L Location D：- Location	ocation A：0.06 ocation B：4.89 ocation C：0.00 D：-
No.4	1807 Hours Ago (63.5mm Rainfall)	24.5	Location A：0.00 L Location B：0.00 L Location C：0.00 L Location D：- Location	ocation A：0.00 ocation B：0.00 ocation C：0.00 D：-
No.5	35 Hours Ago (24.5mm Rainfall)	34.5	Location A：0.00 L Location B：3.91 L Location C：0.00 L Location D：- Location	ocation A：0.00 ocation B：11.3 ocation C：0.00 D：-
No.6	241 Hours Ago (2.5mm Rainfall)	16.5	Location A：0.00 L Location B：0.00 L Location C：0.00 L Location D：0.51 L	ocation A：0.00 ocation B：0.00 ocation C：0.00 ocation D：3.09

Illustration:
Recent Rain Field = Cumulative Rainfall for the Last Precipitation; Exfiltration Efficiency = Exfiltration Amount / Amount of Rain-Fall.

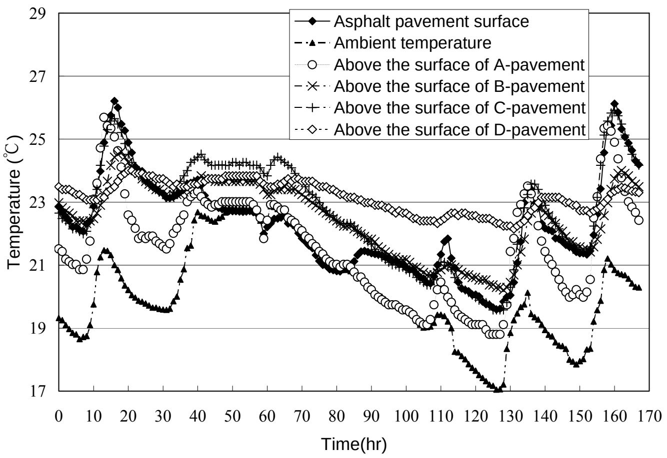

Fig. 14. Surface Temperature Changes in the Experiment Area.

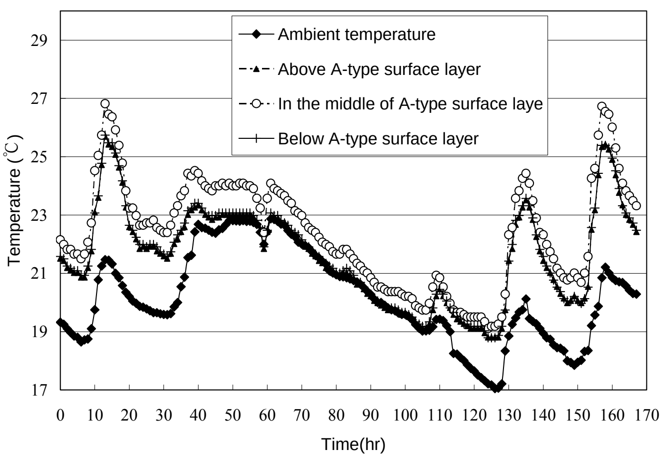

Fig. 15. Temperature Changes of Permeable Pavement Type A.

in Figs. 15 to 18. The observations and analyses are discussed in the following section.

1. Fig. 14 indicates that 36 hours before the rainfall, the pavement temperatures fo r all ty pes of pavement were far above the outdoor ambient temperature. When the ambient temperature at noon was 21^{o}C (Fig. 14, bottom curve), the sidewalk pavement temperature for either Type A or Type C was about 25^{o}C (Fig. 17), which is 4^{o}C higher than the ambient temperature. Asphalt concrete h ad th e highest temper ature, followed b y p avement type A and C.
2. For all pavements except asphalt concrete and pavement type D, the temperature continually dropped for 2 days after the rainfall if the ambient temperature was from 19 to 23^{o}C.
3. Pavement ty pe A has the highest h eat absorption and exothermic cap acity. Pavement type B has a sim ilar lin ear diagram as p avement ty pe A, but not as prono unced thermal properties. Pavement type C has rapid heat absorption but poor exothermic capacity. The geothermometer of p avement type D was embedded in the hole, therefore the measured temperature was easily affected b y the su rrounding air circulation as evidenced by its linear trend.
4. The plots in Figs. 15 to 18 show that a lower geothermometer

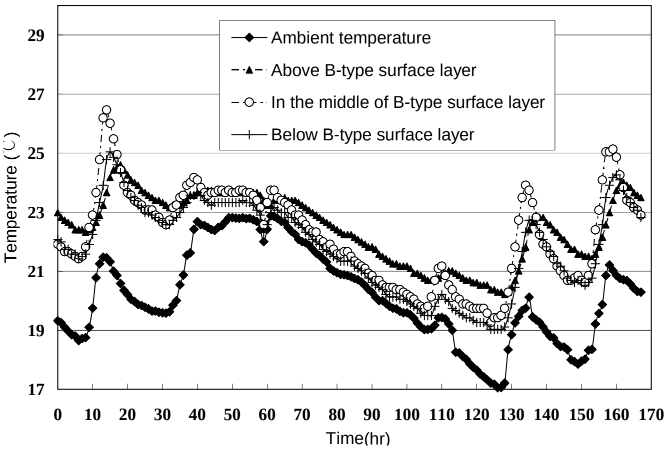

Fig. 16. Temperature Changes of Permeable Pavement Type B.

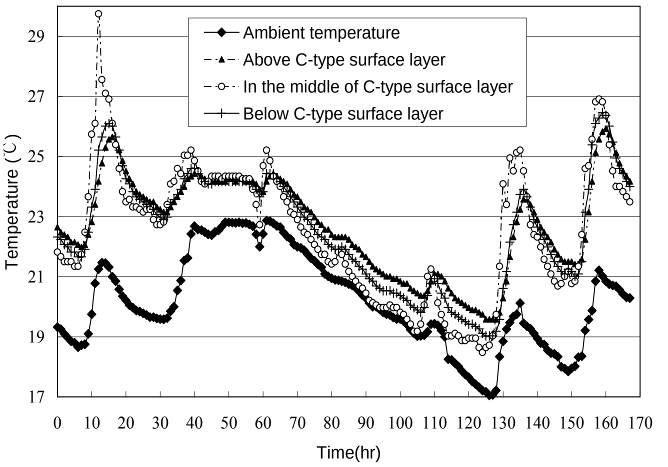

Fig. 17. Temperature Changes of Permeable Pavement Type C.

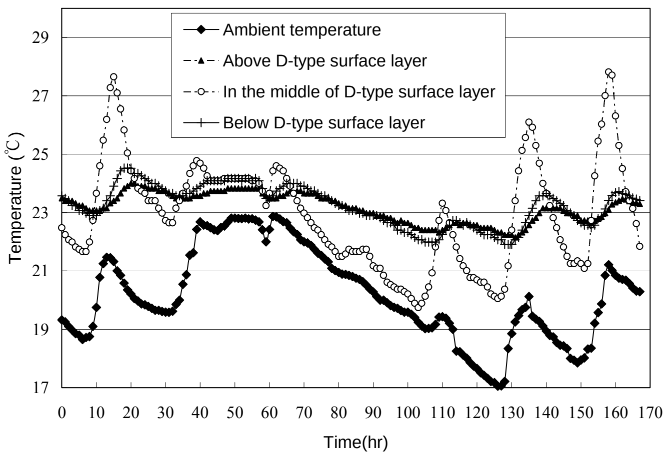

Fig. 18. Temperature Changes of Permeable Pavement Type D.

yielded more obvious oscillation of the measured temperature and elevated heat absorption and exothermic capacities. Besides the installation position, this phenomenon may also be affected by the heat absorption rate and heat storage of the material surrounding the geothermometer.

On-Site Experiment

The surface runoff and the relationship between temperature and soil water content can be evaluated based on the results of the Guelph infiltration meter test and the on-site, measured water retention. These results allow the assessment of the amount of water retained in the well and the infiltration rate.

Water-Retention Test

The objective of the water-retention test is to determine the degree of water retention in the permeable pavement. The results from the long-term monitoring of infiltration, exfiltration, and ground temperature demonstrate that permeable surface paving assists in recharging groundwater and lowering surface runoff. The influence of temperature on the efficiency of these functions can also be evaluated.

The experimental method is to spray a known quantity of water on the permeable surface pavement until the water meter buried in the pavement starts to register readings. As the quantity of water consumed in this experiment is enormous, the experiment cannot be carried out if a local water source is not available – in other words, the experiment cannot be done at all sites.

The first on-site experiment was carried out 144*hrs* (6 days) after the first precipitation (Rainfall No. 1) by adding 26.67*mm*/30*min* of water at Stations B and D. There was a total of 402*mm* precipitation in 162*hrs* for Rainfall No. 1, whereas no water was registered on the water meter 241 *hrs* later. This indicates that 144*hrs* (6 days) after Rainfall No. 1, the surface pavement still retains some water. Hence, the water retention obtained for this period is quite conservative.

The second, on-site experiment was performed by adding 35.56*mm*/40*min* of water at Station B and 80.00*mm*/90*min* of water at Station D. Twenty-seven days before the experiment started there had been no precipitation. This experiment was added mainly to demonstrate that the infiltration/exfiltration amount approaching zero was caused by the clogging of the aqueduct in the pavement at Station D. A similar experiment was also carried out at Station B, and the results are presented in the background information.

1. The results shown in Table 5 indicate that Types A, B, and D permeable pavements have good permeability of 8.9*mm*/10*min*.
2. The results on water retention obtained at Stations B and D during the first experiment show that the permeable pavement maintained its water retaining capability after Rainfall No. 1, which totaled 402*mm* in 162*hrs*.
3. Results of the second experiment done at Stations B and D reveal that, with the same construction time, climate, and pavement structure at the two stations, water flowed out of the pavement at Station D when 35*mm* of water was added, whereas for Station D, when 80*mm* of water was applied, no water was observed to flow out of the pavement.
4. The previous precipitation will influence the current physical condition of the soil, thus affecting the water content and infiltration rate of the pavement. The results of two tests conducted at Station B reveal that the pavement water-retention measures after consecutive clear days and after consecutive rainy days are somewhat different. This observation conforms to the results calculated using the Philip infiltration formulae. The water content in soil, which is enhanced by percolation of rainwater, decreases with increasing soil depth. The soil is saturated

Table 4. Infiltration Efficiency and Surface Runoff Efficiency.

No.	Amount of Rain-fall(*mm*)	Exfiltration Amount(*mm*)	Infiltration Efficiency(%)	Surface Runoff Efficiency(%)
No.1 401.50		Location A：0.81 Location B：10.47 Location C：0.00 Location D：-	Location A：6.5 Location B：8.9 Location C：- Location D：-	Location A：93.5 Location B：91.1 Location C：- Location D：-
No.2 34.	00	Location A：0.27 Location B：3.11 Location C：0.00 Location D：3.07	Location A：74.6 Location B：82.9 Location C：- Location D：80.2	Location A：25.4 Location B：17.1 Location C：- Location D：19.8
No.3 63.	50	Location A：0.04 Location B：3.11 Location C：0.00 Location D：-	Location A：39.6 Location B：44.4 Location C：- Location D：-	Location A：60.4 Location B：55.6 Location C：- Location D：-
No.4 24.	50	Location A：0.00 Location B：0.00 Location C：0.00 Location D：-	Location A：100 Location B：100 Location C：- Location D：-	Location A：0.0 Location B：0.0 Location C：- Location D：-
No.5 34.	50	Location A：0.00 Location B：3.91 Location C：0.00 Location D：-	Location A：72.8 Location B：84.1 Location C：- Location D：-	Location A：27.2 Location B：15.9 Location C：- Location D：-
No.6 16.5		Location A：0.00 Location B：0.00 Location C：0.00 Location D：0.51	Location A：100 Location B：100 Location C：- Location D：100	Location A：0.0 Location B：0.0 Location C：- Location D：0.0

Infiltration Efficiency = (Exfiltration + Water Retention) / Precipitation
Surface Runoff Efficiency = (Amount of Rain-Fall - Exfiltration Amount - Water Retention) / Precipitation

Table 5. Water Retention Experiment.

NO.	Experiment Location	Added Water	Infiltration Efficiency (%)	Exfiltration Amount (*mm*)	Water Retention (*mm*)
1 A		26.67*mm*/30*min* 100		2.48	24.19
1 B		26.67*mm*/30*min* 100		1.57	25.10
2 B		35.56*mm*/40*min* 100		0.42	35.14
2 D		80.00*mm*/90*min*	100 0.00		25.10

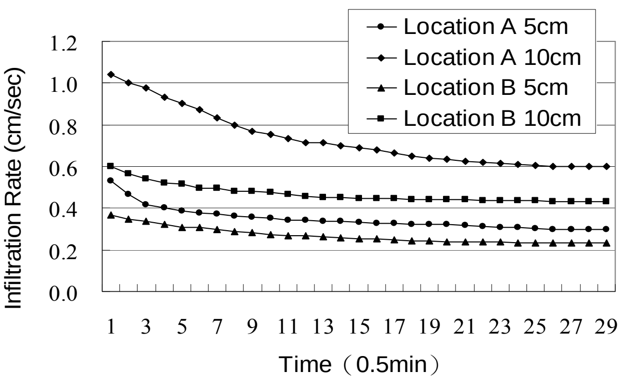

Fig. 19. The Recorded Filtration Rate for Stations A and B.

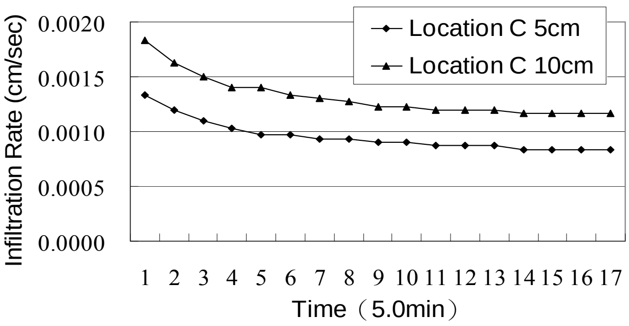

Fig. 20. The Recorded Filtration Rate for Stations.

after the rain, but the moisture is transferred and ultimately leaves entirely.

The Guelph Infiltration Meter Test

The objective of this test is to estimate the steady infiltration rate for each monitoring station, and the results are compared with the long-term monitored precipitation for calculating the surface runoff.

1. Figs. 19 and 20 show that the infiltration rate was maximal during the initial seeping period and gradually decreased to a steady level after some time. This result is the same as those calculated using the Horton infiltration formulae.
2. Table 6 reveals that all monitoring stations except Station C had satisfactory **i**nfiltration **r**ates of more than 1.0×10^{-2} *cm/s.*

Table 6. The Steady-State Infiltration Rate at Various Monitoring Stations.

Experiment Location	Overall Steady-State Infiltration Rate (*cm/s*)
A	2.96×10^{-2}
B	1.82×10^{-2}
C	9.72×10^{-5}
D	3.80×10^{-2}

Note: The Calculated Steady-state Infiltration Rate Using the Double-ring Infiltrometer for Station D.

Results and Discussion

1. The pavement water infiltration rate should be the sum of pavement exfiltration amount and water retention, which are related to the previous precipitation. As no instrument for long-term monitoring of pavement water retention is available, on-site measurement of the pavement water retention was carried out.
2. The results shown in Table 5 indicate that the calculated water retention after several consecutive clear days and after several consecutive rainy days have much discrepancy. Hence, the conservative water retentions are assumed to be 25.10 *mm* for Station B and 24.19*mm* for Station A. Station D experienced a clogged aqueduct and its water-retention measure could not be obtained. However, it has the same pavement structure as Station B, so the water retention of 25.10*mm* for Station B was assumed for Station D. As for Station C, its pavement percolation coefficient was very small, and its water retention in the experimental region could not be evaluated.
3. Table 4 lists the manipulated infiltration efficiency and surface unoff rate, which are obtained based on the comparison of rainfall records listed in Table 3 and the above estimated water retention:

(1) Comparisons of the rainfall intensities shown in Figs. 8 to 13 and the steady-state infiltration rates indicate that, except for Station C, all other stations had 100% infiltration efficiency. However, the percent seepage benefit data listed in Table 4 reveal that, unless the precipitation is light, most seepage efficiencies are less than 80%. This conclusion is different from the aforementioned discussion because, in addition to climate, wind speed, impact of precipitation and other factors, such as the extremely intense instantaneous precipitation, low soil permeability, and limited water-storing capacity for the permeable concrete layer will also cause the observed discrepancy. Station C, which had low permeability for the surface layers and hence no rapid percolation, will not be discussed. At Station D, the rainwater could not be discharged because of clogged openings and strong rainfall (the JW Structural Pervious Air-Circulated Aqueduct Concrete Pavement was used at this station). The plastic pipe structure above the surface layer and the openings are easily clogged by soil or leaves, thus contributing to its poor water-discharging capability.

(2) The seepage benefit and surface runoff rates for Stations A, B, and D listed in Table 4 show that the proposed permeable pavement is effective in recharging groundwater and suppressing surface runoff.

4. Because no instrument was installed for measuring the time-dependent surface runoff for the test region with permeable pavement, the peak surface runoff, actual total surface runoff, and the peak lag time cannot be evaluated and compared with the modeling results.
4. The estimated water retention for the permeable pavement installed at Station B (Table 5) from dry to saturated conditions is 35.14 *mm* of precipitation. Comparing this value and the thermal energy efficiency reveals that the permeable pavement will continually reduce the surface temperature for 2 days under conditions of 35.14 *mm* of precipitation and 19-23 ^{o}C ambient temperature.

Conclusions

This is the pioneer study of water permeable pavement in Taiwan, and the following can be concluded:

1. The thickness of permeable pavement must be determined by considering mechanical conditions such as soil strength and traffic, and by hydrological concerns such as permeability and rainfall intensity. On-site boring tests must be conducted to determine whether the permeable pavement can be constructed. The selection of permeable material must include consideration of the foundation condition, allowable loadings, rainfall intensity, and maintenance concerns.
2. As for the hydrology research results, the water-permeable pavement has significant benefits in suppressing rainstorm runoff and increasing the underground water influx. Specifically, when the amount of rainfall is less than 35 *mm*, infiltration efficiency exceeds 80%.
3. The permeable pavement begins to show the effect of reducing the temperature of the ground surface after the rain. Its cooling capability and duration mainly depend on the ambient temperature and the water retention of the permeable pavement. Under wet conditions, the temperature of permeable pavement can keep dropping for two days when the ambient temperature is from 19 to 23^{o}C.
4. On-site measurement of water retention and the Guelph infiltration meter test show that the permeation time and rate are affected by the previous rainfall. This observation conforms to the calculated results using the Philip and Horton infiltration formulae.
5. During clear days, the permeable pavement surface temperature will change depending on the capability of the material to absorb and release heat. Permeable pavement has surface temperature similar to the temperature of asphalt surface - hence, it is not effective at reducing the ground surface temperature.
6. After precipitation, the permeable pavement is effective in reducing the ground surface temperature. The capability and duration of reducing the ground surface temperature depend on solar irradiation temperature and the water content in the permeable material. Under saturation conditions, the temperature drop can reach 8 ^{o}C if the ambient temperature exceeds 30^{o}C (but only for 1 day).

References

1. Oke, T.R., (1982). The Energetic Basis of the Urban Heat Island, *Quarterly Journal of the Royal Meteorological Society*, Vol. 108, pp. 1-24.
2. Ghafoori, N. and Dutta, S., (1995). Development of No-Fines Concrete Pavement Applications, *Journal of Transportation Engineering*, *ASCE*, 121(3), pp. 283-288.
3. Haselbach, L. M. and Freeman, R.M., (2006). A Vertical Porosity Distributions in Pervious Concrete Pavement, *ACI Materials Journal*, 103(6), pp. 452-458.
4. Jayasuriya, L.N.N., Kadurupokune, N., Othman, M., and Jesse, K., (2007). Contributing to the Sustainable Use of Storm Water: The Role of Pervious Pavements, *Water Science and Technology*, 56(12), pp. 69-75.
5. Yang, J. and Jiang, G., (2003). Experimental Study on Properties of Pervious Concrete Pavement Materials, *Cement and Concrete Research*, 33(3), pp. 381-386.
6. Akhtaruzzaman, A.A. and Hasnat, A., (1983). Properties of Concrete Using Crushed Brick as Aggregate, *Concrete International*, 5(2), pp. 58-63.
7. Khaloo, A.R., (1994). Properties of Concrete Using Crushed Clinker Brick as Coarse Aggregate, *ACI Materials Journal*, 91(4), pp. 401-407.
8. Poon, C.S. and Chan, D., (2006). Paving Blocks Made with Recycled Concrete Aggregate and Crushed Clay Brick, *Construction and Building Materials*, 20(8), pp. 569-577.
9. Poon, C.S., Kou, S.C., and Lam, L., (2002). Use of Recycled Aggregates in Moulded Concrete Bricks and Blocks, *Construction and Building Materials*, 16(5), pp. 281-289.
10. Valdés, G.A. and Rapimán, J.G., (2007). Physical and Mechanical Properties of Concrete Bricks Produced with Recycled Aggregates, *Informacion Tecnologica*, 18(3), pp. 81-88.